

Dynamic Delaunay tetrahedralizations and Voronoi tessellations in three dimensions

Gernot Schaller¹ and Michael Meyer-Hermann

*Institut für Theoretische Physik, Technische Universität Dresden, D-01062
Dresden, Germany*

Abstract

We describe the implementation of an incremental insertion algorithm to construct and maintain three-dimensional Delaunay triangulations with dynamic vertices using a three-simplex data structure. The code is capable of constructing the geometric dual, the Voronoi or Dirichlet tessellation. A given list of generators is triangulated and volumes as well as contact surfaces of the Dirichlet regions can be calculated. We use three-dimensional simplex flip algorithms, an algorithm for point location that does not rely on the history of the triangulation construction and in addition, we develop a simple method of deleting vertices from an existing three-dimensional Delaunay triangulation which was a difficult problem until now. The dynamics of the triangulation may therefore not only be governed by dynamic vertex positions but also by a changing number of vertices. Such triangulations are of immense importance to determine the neighborhood topology in individually based continuous models. The dual Dirichlet tessellation can be used to solve differential equations on an irregular grid, to define partitions in cell tissue simulations, for collision detection etc. The straightforward generalization to power-weighted Delaunay-triangulations and Voronoi tessellations is outlined.

Key words: Delaunay triangulation, tissue modelling, Dirichlet, Voronoi, flips, point location, vertex deletion, neighborhood

In nearly all aspects of science nowadays simulations of discrete objects underlying different interactions play a very important role. Such an interaction for example could be mediated by colliding grains of sand in an hourglass [1] or – more abstract – the neighborhood question of influence regions (also sometimes called the neighborhood problem). One general method to represent possible two-body interactions within a system of N objects is given by a network which can be described by an $N \times N$ adjacency matrix ν , with its matrix elements $\nu_{ij} = \nu_{ji}$ (undirected graph) representing the interaction between the

¹ Corresponding author, electronic address : `schaller@theory.phy.tu-dresden.de`

objects i and j . However, for most realistic systems the graph defined this way is not practical if one remembers that the typical size of a system of atoms in chemistry can be $\mathcal{O}(10^{23})$, the human body consists of $\mathcal{O}(10^{18})$ cells and even simple systems such as a grain-filled hourglass contain $\mathcal{O}(10^3)$ constituents. Even some reasonable fraction of such systems would be far too complex to be simulated by adjacency matrices. However, in most systems in reality the interactions at work have only a limited range. Physical contact forces such as adhesion for example, can only be mediated between next neighbors. In the example of colliding sand grains in an hourglass it is obvious that the grain i can not instantaneously affect the dynamics of grain j if the grains do not touch. In such systems the adjacency matrix elements ν_{ij} would vanish for all distant grains. A more efficient description of such systems, where interaction is only mediated locally, can be given by a sparse graph, where the adjacency relations between objects moving in their parameter space can be updated using rather simple methods. In the case of solids crystallizing in a certain lattice, the neighborhood relations are a priori known and can be effectively exploited if one considers all deviations from a lattice configuration as small perturbations. For many crystals, this approximation is a very good one. By defining local interactions between the discrete lattice volume elements one can find numerical solutions to differential equations. The method of cellular automata [2] can also be applied to heterogenous systems such as cell tissues [3,4]. Note however, that several adaptations have to be performed in order to account to the different nature of next-neighborship in these systems. In the realistic system of cells in a human tissue for example, the number of next neighbors per cell is neither constant over the cell ensemble nor are the interaction forces. To make things worse, all these parameters become time dependent for dynamic systems. The same holds true in the framework of collision detection.

In this article it is our aim to describe our implementation of a code generating three-dimensional Delaunay triangulations. Delaunay triangulations and their geometric dual – the Voronoi tessellation – have been demonstrated to be suitable tools to model cell tissues [5,6,7]. However, these considerations have been restricted to the two-dimensional case. In three-dimensional space Delaunay triangulations have been applied in the framework of collision detection amongst spherical grains [1].

The generation of two-dimensional (plane) Delaunay triangulations is a well-covered topic, for a review see e.g. [8,9,10]. Such triangulations are widely used for grid generation in finite element calculations and surface generation for image analysis [11]. Since the Delaunay triangulation in general tries to avoid flat simplices, it also produces a good quality mesh for the solution of differential equations [12,13]. The higher-dimensional case however, is much more complicated. For example, three-dimensional triangulations of the same number of points may have different number of tetrahedra [8]. This can be

compensated by using more dynamic data structures that allow for a varying number of simplices such as lists. A more serious problem however, is posed by the fact, that a two-dimensional polygon can always be triangulated, whereas a three-dimensional nonconvex polyhedron may not admit a decomposition in tetrahedra without using artificial (Steiner) points [14,15]. These differences result in the important consequence that not all algorithms can be generalized in a straightforward way from two-dimensional Delaunay triangulations. The maintenance of the triangulation in the case of dynamic (moving) vertices now requires a data structure capable of handling a varying number of simplices in time. Another important problem is the deletion of vertices from a Delaunay triangulation which is simple in two dimensions [16,17] but transforms into a nontrivial problem in higher dimensions, because in three dimensions there exist nonconvex polyhedra (e.g. Steiner's polyhedron) that can not be triangulated.

We have implemented algorithms for both adding and deleting vertices to a three-dimensional Delaunay triangulation that are incremental in the sense that they transform a Delaunay triangulation with n vertices into a Delaunay triangulation with $(n+1)$ or $(n-1)$ vertices, respectively. In addition, we have implemented flip algorithms [1,18,19] to maintain the Delaunay-property of the triangulation in the case of dynamic vertices. These ingredients together allow to provide a code for three-dimensional Delaunay triangulations with both dynamic (i.e. moving) vertices as well as a variable total number of vertices. Such a code is suitable for the detection of neighborhood relations in dynamic cell tissue simulations, where cell proliferation and cell death are essential elements that have not been covered by Delaunay triangulations in three dimensions before. Since for many neighborhood interaction forces (especially in cell tissues), the contact surfaces and volumes of the dual Dirichlet tessellation is of importance, we have also implemented algorithms to compute these values from a given Delaunay triangulation.

This article is organized as follows:

In section 1 we briefly review the concept of the Delaunay triangulation by addressing the basic conventions in 1.1, the elementary topological transformations in a triangulation in 1.2, defining the Delaunay criterion in 1.3 and consider the geometric dual in 1.4 as well as the more technical volume and surface calculation of Voronoi cells in 1.5. In section 2 we describe the actual implementation of the algorithms by presenting the used data structure in 2.1, an incremental insertion algorithm in 2.2, a point location algorithm in 2.3, the used flip algorithms in 2.4 and close with a description of an algorithm for incremental vertex deletion in 2.5. In section 3 we analyze performances of the incremental insertion algorithm in 3.1, the incremental deletion algorithm in 3.2, the transformation of slightly perturbed Delaunay triangulations into Delaunay triangulations in 3.3, and finally consider the performance of a

combination in 3.4. We will close with a summary in section 4.

1 The Delaunay Triangulation

1.1 Conventions

For the sake of clarity, the illustrations in this article will be two-dimensional, unless noted otherwise. Following the notation in the literature [19,18] we denote by the term vertex a position² in three-dimensional space. By an n -simplex in \mathbb{R}^d ($n \leq d$) we understand the convex hull of a set T of $n + 1$ affinely independent vertices, which reduces in the three-dimensional case to tetrahedra (3-simplices), triangles (2-simplices), edges (1-simplices) and vertices (0-simplices). Every n -simplex has a uniquely defined n -circumsphere. Recall that a tetrahedron is bounded by four triangles, six edges and four points in three dimensions. These ($n \leq d$)-simplices σ_U – formed by the convex hull of a subset $U \subseteq T$ – are also called faces of T . Since we will work in three dimensions, we will shortly denote 3-simplices by the term simplex. A collection of these simplices \mathcal{K} is called a *simplicial complex* if:

- The faces of every simplex in \mathcal{K} are also in \mathcal{K}
- If $\sigma_T \in \mathcal{K}$ and $\sigma_{T'} \in \mathcal{K}$, then $\sigma_T \cap \sigma_{T'} = \sigma_{T \cap T'}$.
(the intersection of two simplices is at most a face of both, the simplices are disjoint)

In numerical calculations with dynamic vertices the above criterion can be destroyed: A vertex might move inside another simplex thus yielding two n -simplices whose intersection is again an n -simplex. We will refer to this situation as an invalid triangulation. To be more exact, a triangulation is defined as follows. If S is a finite set of points in \mathbb{R}^d , then such a simplicial complex \mathcal{K} is called a *triangulation* of S if

- each vertex of \mathcal{K} is in S
- the underlying space of \mathcal{K} is $\text{conv}(S)$

By the degree of a vertex in a triangulation we will denote the number of simplices in the triangulation containing the vertex as endpoints. Furthermore, we will use the terms tetrahedralization and triangulation in three dimensions synonymously, unless noted otherwise.

² If one extends the algorithms towards weighted (regular) triangulations a vertex in addition contains a weight.

1.2 Elementary Topological Transformations

To an existing triangulation in \mathbb{R}^3 several topological transformations can be applied. We will briefly remind the main ideas. For a more detailed discussion see e.g. [18,20]. The discussion basically relies on Radon's theorem (see e.g. [15,18]):

Let X be a set of $d + 2$ points in \mathbb{R}^d . Then a partition $X = X_1 \cup X_2$ with $X_1 \cap X_2 = \emptyset$ exists such that $\text{conv}(X_1) \cup \text{conv}(X_2) \neq \emptyset$.

If X is in general position – meaning that every subset of X with at most $d + 1$ elements is affinely independent – then this partition is also unique. In our case this simply means that [10,19]

- no four points lie on a common plane
- no five points lie on a common sphere

Figure 1 illustrates the idea of Radon's theorem in three dimensions.

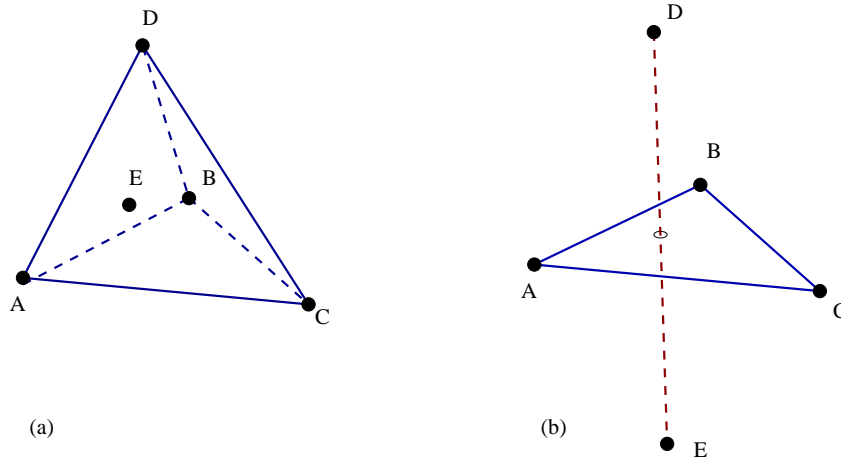


Fig. 1. Illustration of the Radon partition in three dimensions. There are two possible constellations of the 5 points A, B, C, D, E in three dimensions. In (a) the point E lies within the simplex formed by (A, B, C, D), whereas in (b) none of the vertices lies within the simplex formed by the other ones.

From the Radon partition in \mathbb{R}^3 one finds that there exist four possible flips in three dimensions, two for every partition in figure 1. In the case of one vertex being situated within the simplex formed by the remaining four vertices the two possible flips are shown in figure 2. The flip changing the triangulation from 1 to 4 simplices corresponds to adding a vertex to an existing triangulation. Note however, that in practice the inverse transformation may not always be applicable, since the configuration of one vertex (E in figure 2) being the endpoint of exactly four simplices may not be present in a triangulation. This fact – in combination with the existence of non-tetrahedralizable polyhedra in three dimensions – severely complicates the deletion of vertices

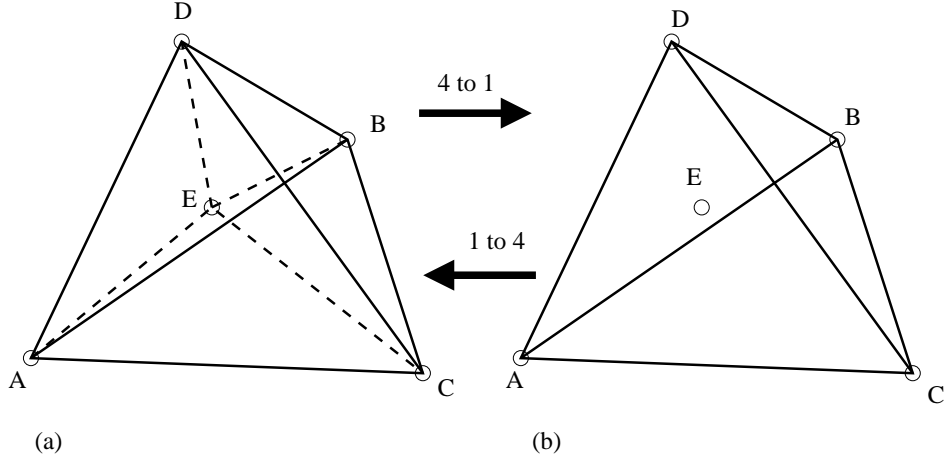


Fig. 2. Three-dimensional illustration of the addition or deletion of a vertex E . In the left picture (a) one has exactly four simplices: (A, B, C, E) , (A, B, D, E) , (A, C, D, E) , (B, C, D, E) , whereas in the right picture (b) the vertex E lies within the simplex (A, B, C, D) . The edges that can principally not be seen from the outside are drawn dashed. Switching between the two configuration corresponds to adding $(1 \rightarrow 4)$ the vertex E to an existing triangulation or deleting it $(4 \rightarrow 1)$, respectively. Note that for these operations to be possible, the point E must lie within the simplex (A, B, C, D) .

from triangulations, see subsection 2.5.

The second partition following from Radon's theorem requires a more careful evaluation, see figure 3. The flips $2 \rightarrow 3$ (and $3 \rightarrow 2$) can only be performed if the polyhedron formed by the five points in \mathbb{R}^3 is convex, otherwise the operation would yield overlapping simplices in the triangulation. The convexity of A, B, C, D, E in figure 3 can be tested by checking if for every edge A, B and B, C and C, A there exists a hyperplane which has the remaining three points $(D, E, A/B/C)$ on the same side [18,19,21].

1.3 The Delaunay Criterion

Every tetrahedron in \mathbb{R}^3 has a uniquely defined circumsphere, if the four vertices do not lie on a common plane (i.e. if the tetrahedron is not flat). Recall that the centers of the circumspheres may lie outside the simplices as is the case with triangles in two dimensions. The Delaunay triangulation is a triangulation where all the simplices satisfy the *Empty-Circumsphere-Criterion*: No vertex of the triangulation may lie inside the circumspheres of the triangulation simplices. Thus, the Delaunay triangulation is uniquely defined if the vertices are in general position, i.e. if no five vertices must lie on a common sphere and no four vertices may lie on a common plane [10]. For an illustration of a Delaunay triangulation see figure 4. Delaunay triangulations have many interesting properties and have been extensively studied in the literature, see

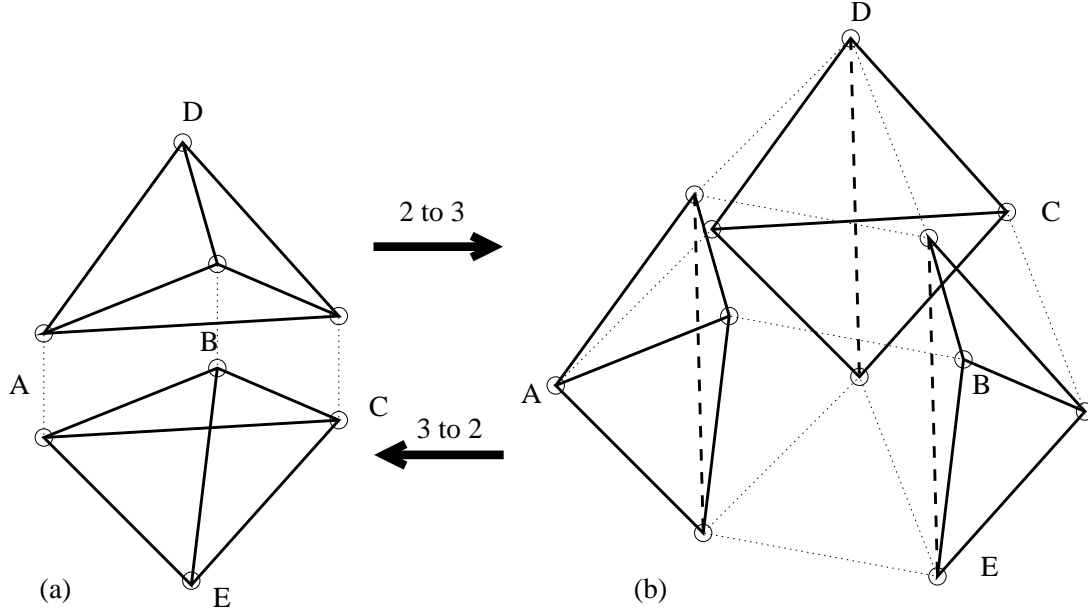


Fig. 3. Three-dimensional illustration of the possible triangulations of five points. In (a) there are two simplices: (A, B, C, D) , (A, B, C, E) , sharing the common triangle (A, B, C) , whereas the right picture (b) consists of three simplices (A, B, D, E) , (B, C, D, E) , (C, A, D, E) . The simplices have been taken apart for clarity and the dotted lines have been drawn to connect the identical points. Edges that are invisible from the outside have been drawn with dashed lines. Note that the flips can only be performed, if the polyhedron (A, B, C, D, E) is convex, since otherwise the flips will result in overlaps with additional neighboring simplices (not shown here).

e.g. [8,9,10,15].

The simplest method to determine, whether a vertex lies outside or inside the circumsphere of a simplex (A, B, C, D) is to solve the associated four sphere equations. However, this problem can be solved more efficiently by adding one more dimension [1,15,19].

Suppose we would like to know whether the vertex E lies in- or outside the circumsphere of the simplex (A, B, C, D) , which we will – without loss of generality – assume to be positively oriented. Then one can proceed as follows: Project the coordinates in \mathbb{R}^3 onto a paraboloid in \mathbb{R}^4 via

$$A = (A_x, A_y, A_z) \rightarrow A^+ = (A_x, A_y, A_z, A_x^2 + A_y^2 + A_z^2). \quad (1)$$

The four points A^+, B^+, C^+, D^+ define a hyperplane in \mathbb{R}^4 . If E is within the circumsphere of (A, B, C, D) , then E^+ will be below this hyperplane in \mathbb{R}^4 and above otherwise. Consequently, the in-circumsphere-criterion in \mathbb{R}^3 reduces to a simple orientation computation in \mathbb{R}^4 , i.e. by virtue of this lifting transformation one finds [1]

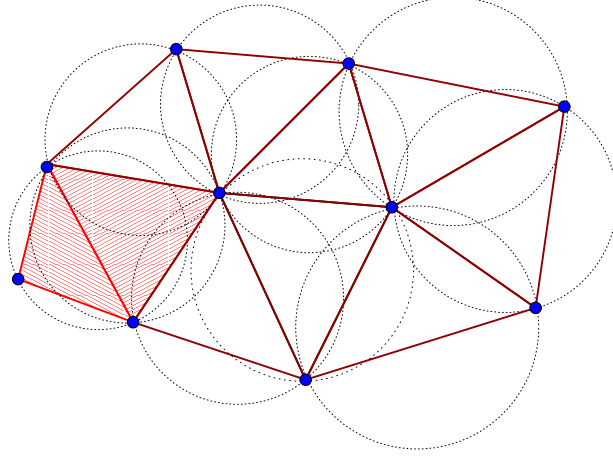


Fig. 4. Two-dimensional illustration of the Delaunay triangulation of 10 vertices. The circumcircles (drawn with dotted lines) of each 2-simplex may not contain any further vertex of the triangulation. If $d + 2$ points lie on a common sphere, their position is also often called degenerate, since there are two possible triangulations satisfying the Delaunay criterion. In this example the two hatched simplices are close to a degenerate position, since their circumspheres do nearly coincide.

$$\begin{aligned}
& \text{in_circumsphere}((A, B, C, D), E) \\
&= \text{oriented}(A^+, B^+, C^+, D^+, E^+) \\
&= \text{sign} \begin{vmatrix} A_x & A_y & A_z & A_x^2 + A_y^2 + A_z^2 & 1 \\ B_x & B_y & B_z & B_x^2 + B_y^2 + B_z^2 & 1 \\ C_x & C_y & C_z & C_x^2 + C_y^2 + C_z^2 & 1 \\ D_x & D_y & D_z & D_x^2 + D_y^2 + D_z^2 & 1 \\ E_x & E_y & E_z & E_x^2 + E_y^2 + E_z^2 & 1 \end{vmatrix} \\
&= \text{sign} \begin{vmatrix} A_x - E_x & A_y - E_y & A_z - E_z & (A_x^2 + A_y^2 + A_z^2) - (E_x^2 + E_y^2 + E_z^2) \\ B_x - E_x & B_y - E_y & B_z - E_z & (B_x^2 + B_y^2 + B_z^2) - (E_x^2 + E_y^2 + E_z^2) \\ C_x - E_x & C_y - E_y & C_z - E_z & (C_x^2 + C_y^2 + C_z^2) - (E_x^2 + E_y^2 + E_z^2) \\ D_x - E_x & D_y - E_y & D_z - E_z & (D_x^2 + D_y^2 + D_z^2) - (E_x^2 + E_y^2 + E_z^2) \end{vmatrix} \quad (2)
\end{aligned}$$

where a positive sign is to be taken as an affirmative answer.

Several algorithms have been developed for the construction of static triangulations [15] as well as for the maintenance of dynamic triangulations [1,20], some of which will be discussed in section 2. The Delaunay triangulation is often used to construct good quality meshes in graphic simulations, engineering, geography and for numerical calculations. In many applications, also the geometric dual, the Voronoi (or Dirichlet) tessellation is of importance, which will be introduced in the following subsection.

1.4 The Geometric Dual: Voronoi Tessellation

The Voronoi tessellation (sometimes also called Dirichlet tessellation) of a set of generators $\{c_i\}$ in \mathbb{R}^d is defined as a partition of space into regions V_i :

$$\begin{aligned} V_i &= \{x \in \mathbb{R}^n : \mathcal{P}_i(x) \leq \mathcal{P}_j(x) \quad \forall j \neq i\} \\ &= \{x \in \mathbb{R}^d : |x - c_i| \leq |x - c_j| \quad \forall j \neq i\}, \end{aligned} \quad (3)$$

where $|\dots|$ denotes the euclidean distance. In other words, the Voronoi cell around the generator c_i contains all points in \mathbb{R}^d that are closer to c_i than to any other generator c_j . Note that this partition is – unlike the Delaunay triangulation – uniquely defined also for point sets that do not fulfill the general position assumption. Voronoi tessellations have many interesting applications in practice – for a survey see e.g. [8] – since they do in some sense describe influence regions (in many real problems the influence of a generator c_i on a point x scales with their euclidean distance).

Consider for instance the two-dimensional example of the post office problem: In a city a certain number of post offices is distributed. Now one could ask the question which region every post office should deliver, such that the postal service in town is as effective as possible. For simplicity one could assume that all post workers have the same carts and the same efficiency and that the density of the streets in the town is very large (such that the carts do not have to take detours). Obviously, then every point being closer to a certain post office i than to any other postoffice $j \neq i$ should be delivered by the post office i . In other words, the influence region of the post office i is given by the Voronoi cell V_i defined in (3).

In 2 dimensions Voronoi cells are convex polygons completely covering the plane, see e.g. figure 5. Note that per definition the Voronoi cells around generators Z_i situated on the convex hull of the point set $Z = \{Z_1, Z_2, \dots, Z_n\}$ will extend to infinity and thus will have an infinite volume. This finding generalizes to arbitrary dimensions: The boundaries between two d -dimensional Voronoi regions V_i and V_j as defined in (3) reduce to the equation for a $d - 1$ hyperplane.

A very simple construction algorithm is to draw connection lines between the generator i and all other generators j of the set. In the half-distance between i and j a perpendicular half-plane generates two half-spaces. If this procedure is performed for all neighbors j then the intersection of all half-spaces containing i defines the Voronoi cell around the generator i . In the case of all generators being distributed on the sites of a regular lattice, this algorithm coincides with that for the construction of the well-known Wigner-Seitz cell in solid state physics [22]. This construction algorithm is extremely slow, but fortunately

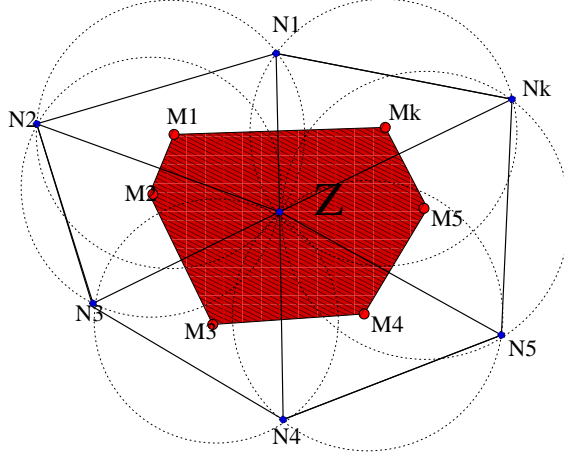


Fig. 5. Two-dimensional Voronoi cell around a generator Z , which is surrounded by other generators N_i . All points within the shaded region are closer to the generator Z than to any other generator. The corners of the Voronoi cell polygons M_i are the centers of the circumcircles (drawn with dotted lines) of the Delaunay triangulation (solid lines) of the generator set.

there are much more efficient ways to construct the Voronoi tessellation.

We would like to summarize some properties of the Voronoi tessellation: In two dimensions, the corners of the Voronoi polygons are the centers of the circumcircles of the triangles contained in the Delaunay triangulation of the Voronoi generators, see figure 5. This reflects the geometric duality between the Delaunay triangulation and the Voronoi tessellation. This duality enables us to focus on the Delaunay triangulation solely in this article. In section 1.5 we will describe how to convert a Delaunay triangulation into the Voronoi tessellation.

The introduction of influence regions also enables the definition of a euclidean neighborhood between vertices: We understand two vertices to be direct neighbors (in the sense that their influence regions touch) if they share a common face in their Voronoi diagram or – equivalently – if they are direct neighbors in the dual Delaunay triangulation, see figure 5.

Consequently, Dirichlet tessellations play a very important role in the detection of collisions between equally sized spheres. Furthermore, the concept of the Voronoi cell can be extended towards influence regions of generators with a varying strength, the weighted Voronoi tessellation [8]. In such extensions, every generator is assigned a weight, i.e. the functions $\mathcal{P}_i(x)$ in (3) are not given by a simple euclidean distance anymore but rather by a function describing the influence strength of the generator i at c_i on x . Thus, a weighted Voronoi region W_i of the generator c_i is defined in n dimensional space via

$$W_i = \{x \in \mathbb{R}^n : \mathcal{P}_i(x) \leq \mathcal{P}_j(x) \quad \forall j \neq i\}. \quad (4)$$

Obviously, the weighted Dirichlet regions can – in contrast to the unweighted case – be empty, e.g. if a vertex with a weak influence is surrounded by strong vertices. The boundaries of these Dirichlet regions are $(n - 1)$ -hypersurfaces defined via

$$S_{ij} = \{x \in \mathbb{R}^n : \mathcal{P}_i(x) = \mathcal{P}_j(x) \quad \forall j \neq i\}. \quad (5)$$

Among many possible choices for weight functions [8,23] we will explicitly mention here the case of power-weighted Voronoi diagrams, also often called the Laguerre complex [1,20]. It is obtained by assigning a weight $\omega_i \in \mathbb{R}$ to every generator c_i , i.e. by replacing $\mathcal{P}_i(x) \rightarrow \mathcal{P}_{i,\omega_i}(x) = (c_i - x)^2 - \omega_i^2$ in (4). The Laguerre cells are then defined via

$$L_i = \{x \in \mathbb{R}^n : (c_i - x)^2 - \omega_i^2 \leq (c_j - x)^2 - \omega_j^2 \quad \forall j \neq i\}. \quad (6)$$

Thinking in terms of distances, the Laguerre cells can be constructed in analogy to the Voronoi diagrams by inserting perpendicular hyperplanes at $\mathcal{P}_i(x) = \mathcal{P}_j(x)$ on the connection line between the generators. These perpendicular planes do lie between the sphere surfaces, if the spheres do not overlap. The advantage is that with this construction, the contact region between two Laguerre cells does not necessarily have the same distance from the two generators. Therefore, the Laguerre tessellation is suitable for collision detection between differently sized spheres [1].

In the power-weighted case one can still show that in three dimensions the Laguerre cells are convex polyhedra, whose corners can be obtained from the weighted centers of the corresponding weighted Delaunay triangulation tetrahedra – where the empty circumsphere criterion is simply replaced by its weighted counterpart [1]. We would like to stress that our assumptions in this article can be generalized to the power-weighted case in a straightforward way.

1.5 Voronoi surfaces and volumes

Within the framework of growth models [20], tissue simulations [6,7] and the solution of partial differential equations on irregular grids [12,13], not only the neighborhood relations in the Delaunay triangulation but also the corresponding Voronoi cell volumes as well as the contact surface between two Voronoi cells may become important. In this section we will describe how to compute these from the corresponding Delaunay triangulation.

We first illustrate the volume computation in two dimensions and then generalize this result to three dimensions. Obviously, to the surface of a Voronoi cell

around a vertex Z every incident simplex σ with $Z \in \sigma$ contributes, see figure 5. In two dimensions every triangle (Z, N_i, N_{i+1}) contributes two surfaces, spanned by the half distances between the vertices $A = 1/2(N_i - Z)$ and $B = 1/2(N_{i+1} - Z)$, and the center of the circumcircle of $R = \text{COC}(Z, N_i, N_{i+1}) - Z$. If (A, B) are positively oriented (which we will furtheron assume without loss of generality), then the oriented 2-volume contribution of the simplex (Z, N_i, N_{i+1}) to the Voronoi cell volume of the vertex Z is given by

$$V_Z = \frac{1}{2} \left(\begin{vmatrix} A_x & R_x \\ A_y & R_y \end{vmatrix} + \begin{vmatrix} R_x & B_x \\ R_y & B_y \end{vmatrix} \right), \quad (7)$$

see also figure 6 for illustration. Obviously, the sum of the three volumes has to equal the total simplex volume $V_Z + V_{N_i} + V_{N_{i+1}} = V_S$. One can show algebraically, that this identity holds true for any R , i.e. also in the interesting case where R being the center of the circumcircle lies outside the triangle as in figure 6. In this case one of the two area contributions in (7) will be negative. Now when considering figure 6 it becomes clear that by adding the oriented volume contributions of all simplices containing the vertex Z one obtains the correct volume for the Voronoi cell around Z .

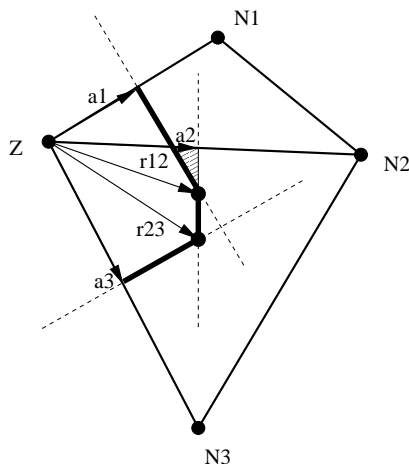


Fig. 6. Volume (area) computation of a two-dimensional Voronoi cell around the generator Z . Here for clarity only two simplices are shown. The first simplex (Z, N_1, N_2) contributes the positive area spanned by (a_1, r_{12}) and the negative area spanned by (r_{12}, a_2) . The second contribution is negative because the center of the circumcircle of (Z, N_1, N_2) is outside the simplex. Most of the negative volume contribution is thus cancelled – up to a small part (hatched region) situated outside the Voronoi cell boundary (thick lines). However, when considering the next simplex (Z, N_2, N_3) the positive contribution spanned by (a_2, r_{23}) cancels with this remaining negative contribution from the first simplex. The last contribution comes from (r_{23}, a_3) and is again positive.

This finding generalizes to three dimensions very well (concerning the surface contribution see [20] for a similar approach). The volume contribution of the

simplex spanned by $(2A, 2B, 2C)$ (with Z being situated at the origin and A, B, C being positively oriented) to the vertex Z is given by

$$V_Z = \frac{1}{6} \left(\left| \frac{1}{2}A, R_{AB}, R \right| + \left| R_{AB}, \frac{1}{2}B, R \right| + \left| \frac{1}{2}B, R_{BC}, R \right| + \left| R_{BC}, \frac{1}{2}C, R \right| + \left| \frac{1}{2}C, R_{CA}, R \right| + \left| R_{CA}, \frac{1}{2}A, R \right| \right). \quad (8)$$

In above equation R denotes the center of the circumsphere of the simplex, and R_{AB} , R_{BC} , and R_{CA} denote the centers of the circumcircles of the simplex facets spanned by (A, B) , (B, C) and (C, A) , respectively. Again the sum over all volume contributions of one simplex (A, B, C, D) returns the simplex volume: $V_S = V_A + V_B + V_C + V_D$. Also in the three-dimensional case the volume contributions of all simplices around one vertex add up to the total Voronoi cell volume around this vertex. These algorithms easily generalize to the power-weighted case: The centers to be computed are now simply the weighted centers of the simplices or triangles, respectively and the half-distance positions between the vertices transform into the positions of equal vertex influence, i.e. where $\mathcal{P}_i = \mathcal{P}_j$.

The contact surface contribution of a simplex containing both vertices can be computed in analogy to the two-dimensional example in figure 6, since the contact surfaces between two Voronoi polyhedra are two-dimensional polygons.

Note that these algorithms do not rely on a specific order of the simplex contributions, since the relative sign of the volumes takes complete care of the correct summation to volumes or surfaces, respectively. Of course, the algorithm leads to a wrong Voronoi cell volume at the boundary, where the Voronoi cells are per definition infinite. However, if the centers of the circumspheres of the simplices at the boundary do not lie outside the convex hull of the triangulation, then the volume summation yields the part of the Voronoi cells which is inside the convex hull. This is desirable for some configurations, such as the solution of partial differential equations [13].

The numerical complexity of the volume computation is linear with the number of simplices surrounding the vertex, whereas the complexity of contact surface calculation between two generators grows linear with the number of simplices containing both generators as endpoints.

We have checked our implementation by using the fact that the sum over all Voronoi cell volumes in a tessellation of the point set T has to equal the sum of the simplex volumes in the dual Delaunay triangulation of T .

2 Algorithms and Implementation

2.1 The Data Structure

As has already been mentioned in the introduction, three-dimensional Delaunay triangulations are much more complicated than in two dimensions. The first difference is that the number of triangulation simplices may vary for a constant number of mobile vertices. This requires a more flexible data structure. However, modern programming languages such as C++ enable a straightforward implementation. Our triangulation basically consists of two data structures:

- a list of the vertices that are to be triangulated
- a list of the 3-simplices (tetrahedra) contained in the triangulation

Both structures are organized in a list to enable for the dynamic movement, addition, deletion of vertices and the corresponding dynamic update of the simplex list, e.g. after the movement of the vertices.

A vertex consists of the x , y and z coordinates³ and – to compute the Voronoi cells efficiently – a list of the incident tetrahedra. A simplex consists of four pointers on vertices and of four pointers on the neighboring simplices. The latter is required by the fact that we use local neighborhood to locate the simplices (see section 2.3) and to extract the facet between two simplices. The neighbors are stored in a defined order that allows to identify the neighbor simplex which is opposite to the vertex A_i , i.e. which does not contain A_i but the other three vertices $A_{j \neq i}$ as endpoints.

The construction of the Delaunay triangulation basically relies on two basic predicates: The determination whether two points lie on the same side of a plane defined by three others and the question whether a point lies in- or outside the circumsphere circumscribing the simplex of four others (enforcement of the Delaunay criterion). By using these two simple predicates the whole triangulation can be built up.

2.2 Incremental Insertion Algorithms

This well-known algorithm answers the question: Suppose we have a Delaunay triangulation with n vertices, how can one find the Delaunay triangulation with an additional arbitrary vertex (thus having $n + 1$ vertices)? Unfortu-

³ Note that for power-weighted triangulations a vertex also contains a weight ω .

nately in Delaunay triangulations the insertion of one new vertex can change the whole triangulation, but this only holds true for some extreme vertex configurations, for some examples see [8]. In practice, the effect of adding a new vertex to a Delaunay triangulation will nearly always be local. Anyhow, the algorithms we describe here can of course also cope with these worst case scenarios.

So let us assume we have a valid Delaunay triangulation with n vertices. Let us furthermore assume that the new vertex lies within the convex hull of the n vertices. Then the updated Delaunay triangulation can be constructed as follows (see figure 7):

- Identify all invalid simplices in the triangulation, i.e. all those containing the new vertex within their circumsphere.
- Collect the external facets of the invalid simplices. (Those are the triangles facing valid simplices.)
- Replace the invalid simplices by new ones formed via combining the external facets with the new vertex.

Sometimes this incremental algorithm is also called *Bowyer-Watson Algorithm* [24,25]. Once all the invalid simplices have been found, its computational cost is very low (linear with the total number of invalid simplices). At first it actually suffices to find the one simplex which contains the new vertex within its convex hull. The remaining invalid simplices can be found iteratively by checking all neighbors of the known invalid simplices for invalidity. Note however, that for weighted triangulations the simplex containing the new vertex within its convex hull is not necessarily invalid, since the weighted circumsphere does not generally contain the complete simplex. This corresponds to the case of an empty Laguerre cell – the vertex therefore has to be rejected. This algorithm is illustrated in figure 7.

The result of this procedure is a Delaunay triangulation with $n+1$ vertices. No flips or further transformations are required, therefore this algorithm turned out to be faster in practice than the incremental *Green-Sibson Algorithm* [24], which needs the simplex containing the new vertex as an input. Then the elementary topological transformation $1 \rightarrow 4$ is performed with this simplex and the resulting (Delaunay-invalid) triangulation is transformed to a Delaunay triangulation by performing $2 \rightarrow 3$ and $3 \rightarrow 2$ flips until all simplices fulfill the Delaunay property.

Obviously, for every incremental algorithm one has to construct an initial Delaunay triangulation first. It is trivial that every triangulation consisting of just one simplex fulfills the Delaunay property. Therefore the idea is to use an artificial large simplex which contains all the data to be triangulated within its convex hull. This simplex can be determined by finding the maximum absolute

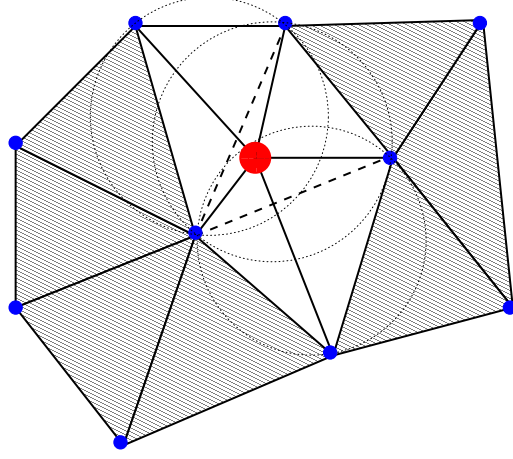


Fig. 7. Two-dimensional illustration of the incremental insertion algorithm. In this example, a new vertex (large point) is inserted into an existing triangulation (not all simplices are shown). Most of the simplices remain valid (shaded region), but 3 simplices (dashed lines) contain the new vertex within their circumspheres (dotted lines). These are replaced by 5 new simplices (solid lines) formed by the new vertex and the external facets (which are simply lines in two dimensions). The resulting triangulation fulfills the Delaunay criterion. In practice as in the above example the overall change to the triangulation will in most cases be local.

value of all coordinates of all vertices, i.e.

$$M = \max_{j=1\dots n, i=1,2,3} x_i^{(j)}, \quad (9)$$

where $x_i^{(j)}$ denotes the i^{th} coordinate of vertex j . Thus, all the data lies within a sphere situated at the origin with radius M . This sphere must be smaller than the insphere of the initial simplex which completely contains the data. One choice for such an initial simplex could be given by the four vertices

$$\begin{aligned} v_1 &= 2M(0, 0, 1) \\ v_2 &= \frac{2M}{3}(2\sqrt{2}, 0, -1) \\ v_3 &= \frac{2M}{3}(-\sqrt{2}, -\sqrt{6}, -1) \\ v_4 &= \frac{2M}{3}(-\sqrt{2}, +\sqrt{6}, -1), \end{aligned} \quad (10)$$

which resemble the CH_4 configuration. Note however, that the maximum norm of the vertices must be known in the beginning. In practice however, one will simply assume a safely large value for M .

2.3 Location of Simplices

In the previous section we have described the incremental insertion algorithm. It should be stressed that the neighbor simplices of a vertex that is to be added to the triangulation are not a priori known. So far, we have not mentioned how to find the first invalid simplex within the triangulation, i.e. the simplex containing the new vertex within its convex hull. Note that our approach of point location only uses the present triangulation and not some kind of construction history (e.g. the so-called Delaunay tree [24] or history dag [26]) or levels of artificial triangulations of subsets [27]. The history approach is rather suitable for triangulations that do not change in time. We are aiming at dynamic triangulations, where the length of such a history stack could not be controlled. Therefore we employ another way of locating the invalid simplices.

The naive method to do this would be to check all simplices in the triangulation. However, for large triangulations this is obviously not practical, since for regular vertex distributions only a small fraction of the simplices will become invalid. Therefore, we perform a directed walk algorithm to locate the first invalid simplex, which is similar to that in [1], though there a more complicated data structure (doubly connected facet-edge list – DCFL) is used. Starting with an arbitrary initial simplex A and a new vertex v to be inserted in the triangulation, we choose one of the four neighbor simplices of A by using the following criterion.

- For all four vertices $a_{i=1,2,3,4}$ of the simplex A check with the new vertex v : Are the vertices a_i and v on different sides of the plane defined by the other three vertices $A_{j \neq i}$?
yes : \implies Jump to the simplex opposite to A_i . no : \implies Check the next vertex A_i .
- If no neighbor simplex is found, the vertex v is contained within the simplex A and the destination is thus reached.

Note that in valid triangulations – where all simplices lie within the convex hull – this hopping algorithm cannot cross the boundary. Obviously, the algorithm can take different pathways (see figure 8) since there may be more than one neighbor fulfilling this criterion. However, since a further test would require much higher effort we stick to this simple criterion. Note also that due to numerical errors the hopping algorithm can produce loops when triangulating regular lattices (such as cubic, ...) that violate the general position assumption. Such pathologic situations can easily be recognized by counting the number of steps and comparing with the overall number of simplices. Possible counter strategies include the selection of another starting simplex or the brutal method of checking all the simplices in the triangulation.

The expected speedup becomes visible if one compares the number of the simplices that have to be checked on a pathwalk to the total number of the simplices in the triangulation, see figure 8. The complexity is directly proportional to the length of the path to be walked – measured in units of traversed simplices. For n uniformly distributed vertices for example, the total number of simplices grows linearly (n) with the number of vertices, whereas the average distance between two arbitrarily selected simplices will grow like $n^{1/3}$. Once the invalid simplex has been found, the average remaining complexity will be constant (in n), i.e. the overall theoretical complexity behaves like $\alpha n^{4/3} + \beta n$ for uniformly distributed points and generalizes in higher dimensions d to $\alpha n^{1+1/d} + \beta n$, see [28].

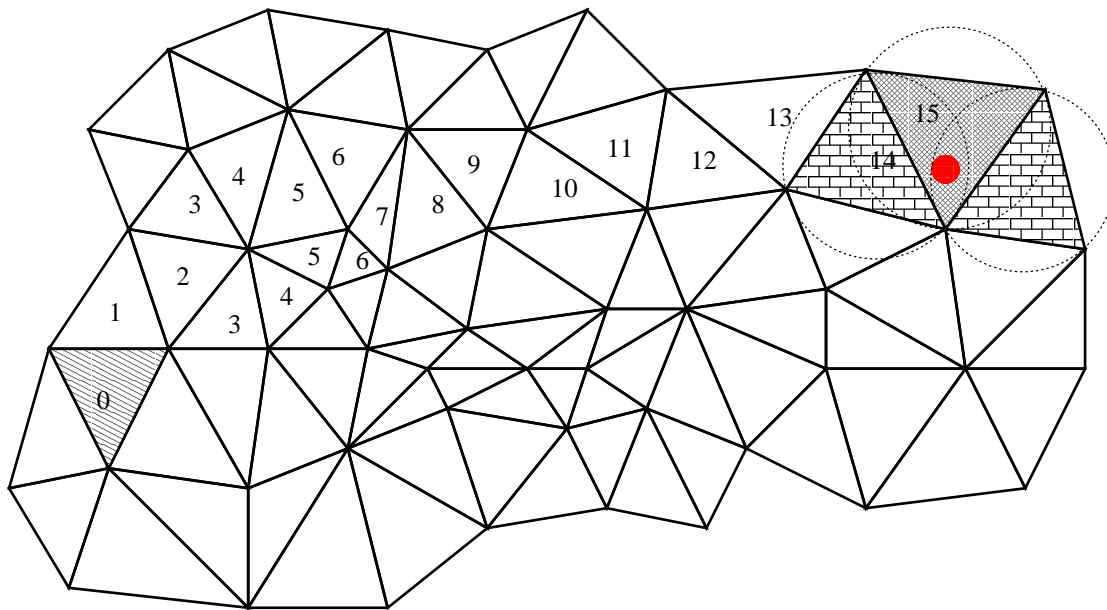


Fig. 8. Two-dimensional illustration of the hopping algorithm in a triangulation (not all simplices are shown). Starting from the hatched initial simplex 0 the algorithm finds its way towards the invalid simplex 15 (cross-hatched) that contains the new vertex (large point). The remaining two invalid simplices (brick-pattern) are found by iteratively checking the neighbors for Delaunay invalidity. Note that there are multiple possible paths as in simplices 2 to 7, which per accident do recombine after an equal number of steps in this example (only two possible paths are shown). The computational time necessary for the walk algorithm is proportional to the number of traversed simplices.

Obviously, the algorithm heavily depends on a good choice of the starting simplex. The method could therefore be improved by checking whether the new vertices lies within a certain subregion and choosing a corresponding starting simplex. In many practical simulations, some neighborhood relations may already be known when building the initial triangulation. Our implementation of the incremental algorithm expects the vertices to be included in some order, such that successive vertices are also very close to each other in the final triangulation and therefore chooses the starting simplex in the walk algorithm

accordingly. For processes as cell proliferation modeled in the Voronoi cell picture, the situation is even better: New cells can be created by cell division which corresponds to the insertion of a new vertex close to an existing one. Consequently, one always has a perfect guess for the starting simplex in these cases.

2.4 *Updating the triangulation*

So far we have not mentioned how to maintain the Delaunay criterion in dynamic triangulations where the vertices are moving and therefore neighborhood relations can change. In this subsection we will only consider the case where the positions of the vertices change in time but their overall number remains constant. This applies to systems such as moving grains – where at small timesteps the dynamics of the vertices is evolved according to the equation of motion that is based on the neighbor vertices given by the triangulation.

As already mentioned, in three dimensions this usually implies a changing number of simplices.

It is evident that in the case of moving vertices the Delaunay criterion may be violated, i.e. after the vertices have moved one may end up with a triangulation that violates the Delaunay criterion. Even worse, if the vertices move too far, e.g. if one vertex moves inside another simplex, the triangulation will become invalid (contain overlapping simplices). This must be avoided by either computing the maximum stepsize (see e.g. section 2.5) or by keeping the displacements safely small. So let us assume here that after vertex movement one is left with a triangulation violating the Delaunay criterion but not containing any overlapping simplices, i.e. a valid non-Delaunay triangulation. If one is interested in Voronoi tessellations or in good quality meshes, then the Delaunay property must be restored. Recomputing the whole triangulation is usually not an option for large data sets, since there is no linear triangulation algorithm available. However, the elementary topological transformations in subsection 1.2 can be exploited to restore the Delaunay criterion. Since we will neither add nor delete vertices in this subsection it is evident that the flips $1 \rightarrow 4$ and $4 \rightarrow 1$ are not necessary. Consequently, the transformations $2 \rightarrow 3$ and $3 \rightarrow 2$ will suffice to transform the given triangulation into a Delaunay triangulation, which has been shown to work in [1,18,19]. Since we rely on a simpler data structure we will reformulate the flip criteria that need to be imposed.

Suppose we want to check and update a list of simplices of a triangulation to transform it into the Delaunay triangulation. This list of simplices can either be the complete triangulation, or only a small subset, e.g. the simplices

incident to one vertex which has moved or the simplices incident to a new vertex that has been inserted via the Green-Sibson algorithm. By analyzing the meaning of neighborhood in Voronoi diagrams and Delaunay triangulations one finds that only two situations can occur: The vertex v_i can either approach the vertex v_j , such that a previously non-existent neighborhood entry between v_i and v_j must be created (their two Voronoi cells share a common face) or the vertex v_i departs from the vertex v_j so far that a previously existent neighborhood entry must be removed, the Voronoi cells do not touch anymore.

With a glance at figure 3 one can see that the flip $2 \rightarrow 3$ effectively creates a neighborhood connection, whereas the flip $3 \rightarrow 2$ destroys it. Our simple data structure enables a convenient calculation of the flip criteria in three dimensions in subsection 1.2. The main advantage of the flip algorithm is that it is – in average – linear in the number of simplices which – in most practical applications – is also linear with the number of vertices.

We iterate through the list of simplices and perform checks among every simplex (the active simplex) and its neighbors (the passive simplices) for the flips $2 \rightarrow 3$ and $3 \rightarrow 2$. If the flip criterion is fulfilled, then the flip is performed – thus changing the total number of simplices. The new simplices are inserted at the end of the list of simplices to be checked and are therefore checked again at a later time. This algorithm terminates if the end of the list of simplices is reached.

Given two simplices S and its neighbor N_i , the flip $2 \rightarrow 3$ is performed if the following two conditions are met:

- The opposing vertex of the neighbor N_i lies within the circumsphere of the simplex S .
- The five points $S_A, S_B, S_C, S_D, N_{opp}^i$ form a convex polyhedron, where N_{opp}^i is the one vertex in N_i that is not part of S .

In the last criterion it suffices because of Radon's theorem to check whether the edges of the common triangle (without loss of generality (S_A, S_B, S_C)) are convex with respect to the other two points (S_D and N_{opp}^i) [18,19]. It does not matter whether one asks if N_{opp}^i lies within the circumsphere of S or if $S_{opp(N_i)}$ lies within the circumsphere of N_i . In this context, we also prefer to talk about active (S) and passive (N_i) simplices.

The criterion for the flip $3 \rightarrow 2$ can be written as follows: Given the simplex S and two of its neighbors N_i and N_j , the flip $3 \rightarrow 2$ is performed if the following conditions are met:

- The simplex N_i is a neighbor of N_j .
- The neighbor pairs $(S, N_i), (S, N_j)$ and (N_i, N_j) violate the Delaunay criterion.

Note however, that for these flips to be possible, all simplices must be disjoint, i.e. the intersection of two simplices may at most be a triangle. Flips cannot be used to recover from a triangulation with intersecting simplices. In other words, the triangulation must be valid for the flips to be performed. This becomes an issue when choosing the timestep size for the vertex dynamics, compare subsection 2.5.

2.5 *Deletion of Vertices*

In many problems (e.g. mesh generation) the deletion of vertices from a Delaunay triangulation is not of great importance, since there is no great advantage other than a negligible gain in efficiency. However, if the triangulation is used for example for growth models based on Voronoi/Laguerre tessellations, vertex deletion may become important if the model also includes the vanishing of cells (e.g. apoptosis). Obviously, the flip $4 \rightarrow 1$ (see figure 2) effectively deletes a vertex from the triangulation by removing all simplices containing this vertex as endpoint. This transformation however, can only be applied to vertices whose degree is four – such a configuration could be achieved by flipping. In this article, we will follow another idea.

Several algorithms have been developed to manage the deletion of vertices in two dimensions, see e.g. [16,17]. As has already been argued, there exist fundamental differences between the twodimensional and the higherdimensional case. Simply removing a vertex together with its incident simplices leaves a star-shaped hole in the triangulation, which is not necessarily convex. The non-convexity of this hole poses a problem for vertex deletion in dimensions larger than two. Unlike in two-dimensional case, where a star-shaped polygon always admits a triangulation which can be transformed by flips into the Delaunay triangulation [16,17] in three dimensions a star-shaped polyhedron may not admit a tetrahedralization. The simplest example for such a polyhedron is Schönhardt’s polyhedron [14], reported among others in [29]. We think that the algorithm presented in [17] can therefore not be easily generalized to higher dimensions. This algorithm only attempts to fill the hole created by deleting a vertex, it does not treat the rest of the triangulation, which may be affected by vertex deletion in three dimensions (compare the end of the section).

Another approach that uses the history of the triangulation is given in [30], where the history is used to reconstruct the triangulation such that the vertex has never been inserted. Since this algorithm uses flips, it might also correctly handle the rest of the triangulation. Again, in our approach we did not want to use some kind of history, since for dynamic triangulations there is no way to control the size of the history.

The basic idea of our approach to delete a vertex is to move it towards its nearest neighbor in several steps, each followed by a sequence of flips $2 \rightarrow 3$ and $3 \rightarrow 2$ restoring the Delaunay property, until the simplices between the two vertices are very flat and can be clipped out of the triangulation without harming its validity. In some sense we project the problem of vertex deletion on the already presented algorithm for vertex movement. Figure 9 illustrates the idea of the algorithm.

The main questions to be answered all reduce to the problem of the stepsize. How far can a vertex v_i be moved into a certain direction without damaging the triangulation, i.e. without creating overlapping simplices? If the vertex v_i penetrates another simplex, the orientation of at least one of its surrounding simplices will change. Therefore one can derive a stepsize criterion by demanding that the orientation of the simplices incident to v_i may not change sign. We define the pseudo-orientation of a simplex $S_i = (A^{(i)}, B^{(i)}, C^{(i)}, D^{(i)})$ as follows:

$$\begin{aligned} \mathcal{V}_0^{(i)} &= \begin{vmatrix} A_x^{(i)} & A_y^{(i)} & A_z^{(i)} & 1 \\ B_x^{(i)} & B_y^{(i)} & B_z^{(i)} & 1 \\ C_x^{(i)} & C_y^{(i)} & C_z^{(i)} & 1 \\ D_x^{(i)} & D_y^{(i)} & D_z^{(i)} & 1 \end{vmatrix} \\ &= \begin{vmatrix} A_x^{(i)} - B_x^{(i)} & B_x^{(i)} - C_x^{(i)} & B_x^{(i)} - D_x^{(i)} \\ A_y^{(i)} - B_y^{(i)} & B_y^{(i)} - C_y^{(i)} & B_y^{(i)} - D_y^{(i)} \\ A_z^{(i)} - B_z^{(i)} & B_z^{(i)} - C_z^{(i)} & B_z^{(i)} - D_z^{(i)} \end{vmatrix}. \end{aligned} \quad (11)$$

In the second line we have reordered the terms such that the vertex to be moved is in the first column. In fact, this is – up to a factor of $1/6$ – the signed volume of the simplex S_i . Now suppose that one of the vertices – without loss of generality we have chosen A – is moved along the direction of Δ , i.e. $A \rightarrow A' = A + \lambda_i \Delta$ with $\lambda \in \mathbb{R}$ and $\Delta = (\Delta_x, \Delta_y, \Delta_z)$. Then the new pseudo-orientation is obtained via

$$\mathcal{V}_1^{(i)} = \mathcal{V}_0^{(i)} + \lambda_i \begin{vmatrix} \Delta_x & B_x^{(i)} - C_x^{(i)} & B_x^{(i)} - D_x^{(i)} \\ \Delta_y & B_y^{(i)} - C_y^{(i)} & B_y^{(i)} - D_y^{(i)} \\ \Delta_z & B_z^{(i)} - C_z^{(i)} & B_z^{(i)} - D_z^{(i)} \end{vmatrix}. \quad (12)$$

If the orientation of the simplex $S_i = (A_i, B_i, C_i, D_i)$ is not allowed to change one has found an upper bound for λ_i via

$$\lambda_i(S_i) = \frac{\left| \left(\mathcal{V}_0^{(i)} \right) \right|}{\text{abs} \begin{vmatrix} \Delta_x & B_x^{(i)} - C_x^{(i)} & B_x^{(i)} - D_x^{(i)} \\ \Delta_y & B_y^{(i)} - C_y^{(i)} & B_y^{(i)} - D_y^{(i)} \\ \Delta_z & B_z^{(i)} - C_z^{(i)} & B_z^{(i)} - D_z^{(i)} \end{vmatrix}}. \quad (13)$$

Of course this check has to be done for all simplices incident to the moving vertex A , i.e. with

$$\lambda = \min_{S_k: A \in S_k} \lambda_k \quad (14)$$

one has an overall measure of the maximum stepsize of A in the direction of Δ . If $\lambda > 1$, then the vertex can simply be moved along the complete path $(\Delta_x, \Delta_y, \Delta_z)$, whereas if $\lambda < 1$ the vertex A can only be moved by a fraction of that pathway. Note that $\lambda = 0$ will correspond to $\left| \left(\mathcal{V}_0^{(i)} \right) \right| = 0$ for at least one i meaning that A would be incident to a simplex with a vanishing volume. This is not the case in valid triangulations but nevertheless poses a problem with rounding errors. Let us furthermore define A' to be the nearest neighbor of A . These vertices will have a certain number of simplices in common. For the remaining simplices we define the quantity λ_{REST} in analogy to λ via

$$\lambda_{\text{REST}} = \min_{S_k: A \in S_k, A' \notin S_k} \lambda_k \quad (15)$$

Thus, our algorithm for deleting a vertex A can be summarized as follows:

- (1) Find the nearest neighbor vertex A' .
- (2) *repeat*
 - set $\Delta = A' - A$
 - determine $\lambda = \min_{S_k: A \in S_k} \lambda_k$
 - determine $\lambda_{\text{REST}} = \min_{S_k: A \in S_k, A' \notin S_k} \lambda_k$
 - if $\lambda_{\text{REST}} \leq 1.0$ move $A \rightarrow A + \alpha \lambda \Delta$ with $\alpha < 1$ and update the simplices surrounding A with flips to restore Delaunay property
 - until* $\lambda_{\text{REST}} > 1.0$
- (3)
 - delete the simplices containing both A and A'
 - replace A by A' in all simplices surrounding A
 - set the correct neighborhood relations in these simplices
 - update the simplices incident to A' with flips

The simplices containing both A and A' will change their orientation in the last step, since their volume vanishes when A and A' merge. However, since these simplices are deleted anyway, their orientation does not need to be maintained within this last step. The orientation of the simplices containing A but not A' (described by λ_{REST}) however, needs to be maintained, since these simplices

will not be deleted afterwards. Therefore, the quantity λ_{REST} should be the criterion for the last vertex step, whereas λ accounts for the maximum length of the previous steps.

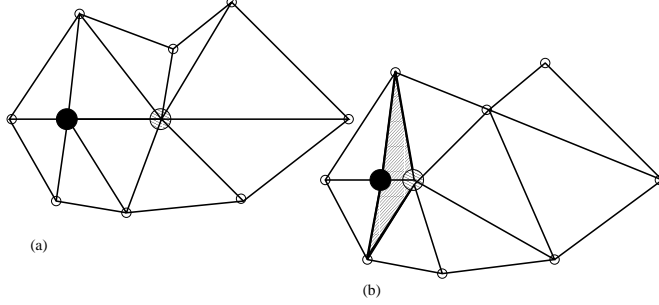


Fig. 9. Two-dimensional illustration of vertex deletion from a Delaunay triangulation. In part a, the vertex to be deleted (large hatched point) is moved in several steps followed by flips restoring the Delaunay property towards its closest neighbor (large solid point), until the inner simplices (shaded region) can be safely deleted (part b). The two vertices are simply merged and the remaining opposing simplices are connected as neighbors. Finally, the Delaunay criterion is again restored by using flips.

The possibility of the moving vertex colliding with another vertex is not given, because we are moving the vertex towards its nearest neighbor – there is no vertex in the Delaunay triangulation that can be closer than the nearest neighbor, therefore such a case cannot happen. Another problem is posed by rounding errors in (13): If the numerator becomes very small – i.e. if one has simplices with an extremely small volume or very skinny simplices, then λ may tend to assume very small values. Rounding errors are then likely to happen as well. This problem can be weakened by using exact arithmetics when computing (13) or – when working with random data – by distributing the data over a larger region of space (larger simplices).

We have run several tests on the deletion algorithm by first triangulating a number of points and then deleting all the points one by one. Before we applied the deletion algorithm we determined the simplices surrounding the hole that would be created by naively removing the vertex without triangulation – roughly speaking, we identified the next-next neighbor simplices. After the deletion algorithm had been applied we checked if these simplices were still existent in the final triangulation. It turned out that over 10 sample test runs of a 1000 uniformly distributed points in about $25.3 \pm 0.8\%$ (1 standard deviation) of the cases the final triangulation did not contain all of the next-next neighbor simplices – in other words: the rest of the triangulation was affected as well! This confirms that deletion algorithms in more than two dimensions have to treat more than the simplices incident to the deleted vertex and that a straightforward generalization of algorithms working in two dimensions may fail.

3 Performance

To test our implementation, we performed calculations on a 1.533 GHz AMD Athlon processor with 1 GByte of RAM. The code has been compiled using the GNU g++ compiler with compiler optimization set. The times were then obtained using the `clock()` command. The seed values of the random number generator have been determined using the system time. In all test runs, the data consisted of 64-bit double variables.

3.1 Incremental Insertion Algorithm

The algorithmic complexities of the walk algorithm and of the Green-Sibson algorithm have been extensively studied [18]. Here we have studied the computation time in dependence of the number of points to be triangulated. Test runs were performed for different configurations of points ranging from 25000 to 1000000. The variation of the results was extremely small, that's why no statistical error bars are given.

In a first series of runs, we considered a slightly perturbed cubic lattice with the average lattice constant $a = 1.0$, see figure 10. As a starting simplex for the simplex walk we always took a simplex in the center of the cubus. The theoretical algorithmic complexity of $\alpha_c N^{4/3} + \beta_c N$ is in complete agreement with the simulation. In a second test run, we took the same lattice configuration but improved the walk algorithm by giving a guess for the simplex walk. This guess was chosen to be good within the cubus (i.e. good for all points within the cubus) and bad at the surface of the cubus. For large numbers of points – where the ratio between vertices at the boundary of the cubus and the total number of vertices in the cubus becomes small – we find a linear algorithmic complexity, as is expected if the cost for simplex location becomes constant. The triangulations of cubic lattices in three dimensions are known to produce bad quality simplices (called slivers) and therefore a larger number of simplices. To compare with a uniform random distribution we triangulated different numbers of points within the cubus $[-1.0, +1.0] \times [-1.0, +1.0] \times [-1.0, +1.0]$. A much better behaviour of the algorithmic complexity is found. However, since for random data no guess for the simplex walk can be given, the algorithmic complexity remains $\alpha_r N^{4/3} + \beta_r N$ – though with $\alpha_r < \alpha_c$ and $\beta_r < \beta_c$. Furthermore, figure 10 shows that the running times with our simple data structure are competitive with the more sophisticated three-dimensional DCFL data structure [1], and other available code [19], where the used algorithms code scale similiarly on random data.

It is evident that the incremental insertion of data points depends on the

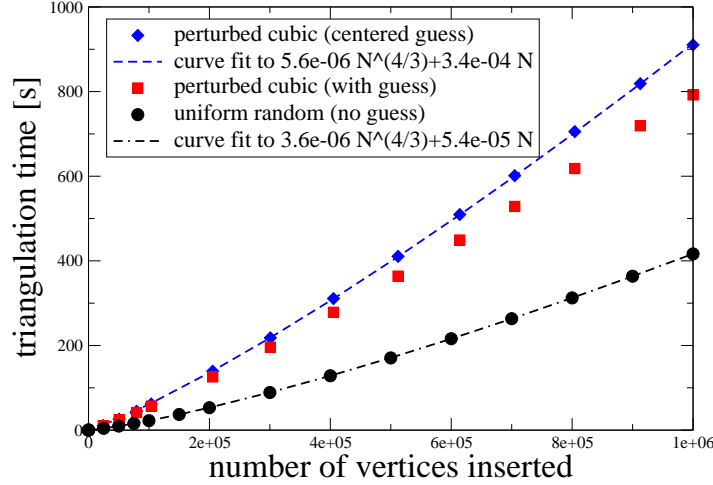


Fig. 10. Times necessary for the tetrahedralization of different point numbers for different distributions. In the case of a cubic lattice without guess the calculation time is largest because the simplex location's algorithmic complexity is $N^{1/3}$ and because the triangulation of cubic lattices produces many slivers. In the case of the points distributed on (perturbed) lattices, the cost of the simplex location can be reduced to constant by giving a good first guess. In the case of randomly distributed points, both the simplex location and the update of the triangulation are much faster than in the cubic lattice – provided no guess is given. Therefore the overall algorithmic complexity is $\alpha_r N^{4/3} + \beta_r N$. Note that when tetrahedralizing even larger point sets, the random distribution will finally be worse than cubic distribution with a good guess at some number of points.

choice of the initial simplex. Figure 11 shows the increase in the average number of hopping steps necessary for the location of the invalid simplices in a triangulation of uniformly distributed points. The expected $n^{1/3}$ relation is found.

3.2 Incremental Deletion Algorithm

In simulation of growth models it will often be necessary to delete vertices from a Delaunay triangulation. It turns out, that vertex deletion is more efficient than vertex insertion, at least for larger point sets. This is mainly due to the fact that no simplex walk is necessary, since no simplices have to be located, as the simplices incident to the deleted vertex are already known. Furthermore, one would expect the average algorithmic complexity of vertex deletion to be constant (i.e. not to depend on the total number of points). In this experiment we have first created a Delaunay triangulation and deleted it afterwards by removing point by point. Again, the mean out of ten test

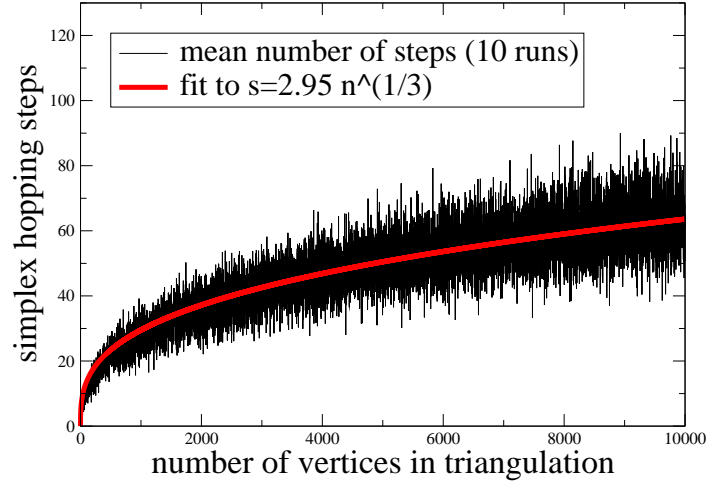


Fig. 11. The number of necessary steps starting from an arbitrary simplex in the triangulation towards another arbitrary simplex scales like $n^{1/3}$. Shown is the mean out of ten runs.

runs has been calculated. Figure 12 gives an impression of the expected linear relationship.

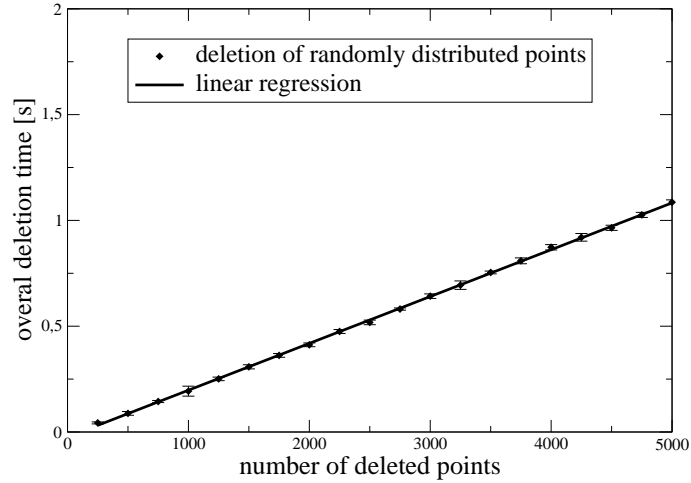


Fig. 12. Shown are the calculation times necessary for the deletion of different numbers of points. The expected linear relation is found. Furthermore, vertex deletion is much more efficient than vertex insertion, if in the latter case no good guess for a start simplex is provided.

3.3 Restoring the Delaunay property

A simulation hosting dynamic vertices will be especially sensitive on the cost of checking all simplices for Delaunay invalidity and restoring the Delaunay property. Recall that retriangulation is usually not an option for larger data sets. We have triangulated a varying number of points and moved these points by a slight step in a random direction. Afterwards the Delaunay property was restored (with a few hundred $2 \rightarrow 3$ or $3 \rightarrow 2$ flips. As is expected for randomly distributed point sets, the complexity behaves linear in the number of points, see e.g. figure 13. By comparing figure 13 with figure 10 one finds that restoring

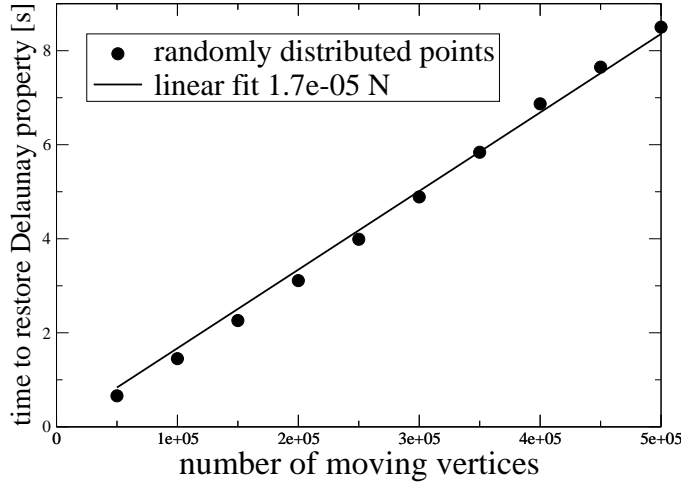


Fig. 13. Shown are the calculation times necessary for the restoration of the Delaunay criterion after the vertices have moved. The expected linear relation is found.

the Delaunay criterion in a slightly perturbed Delaunay triangulation is much faster than recomputing the whole triangulation.

3.4 Mixed algorithms

To check whether a simulation can cope with a varying number of dynamic vertices, we combined the algorithms on vertex insertion, vertex deletion and vertex movement. For different numbers of uniformly distributed vertices 100 time steps have been performed. In each time step, with probability $p = 0.5$ an arbitrary vertex was deleted from the triangulation and with probability $p = 0.5$ a random vertex was inserted. Afterwards all the vertices were moved by a small deviation followed by the restoration of the Delaunay criterion. If

in average a constant number of vertices are deleted or inserted per timestep, we can expect a linear behaviour of the code as is shown in table 3.4.

Table 1

Code performance for different numbers of vertices. In every run, 100 timesteps have been performed. In each timestep, with probability $p = 0.5$ either an old vertex was deleted or a new vertex was inserted into the triangulation (second and third columns). Then all the vertices were moved by a small amount and the flips necessary to restore the Delaunay criterion have been counted – the fourth column does not include the flips necessary for the deletion process. In the last column, the calculation time per timestep is given.

| points | deletions (total) | insertions (total) | flips (total) | one timestep [s] |
|--------|-------------------|--------------------|---------------|------------------|
| 20000 | 59 | 41 | 426 | 0.26 |
| 40000 | 51 | 49 | 1098 | 0.54 |
| 60000 | 52 | 48 | 2067 | 0.84 |
| 80000 | 46 | 54 | 2749 | 1.15 |
| 100000 | 42 | 58 | 3521 | 1.47 |
| 120000 | 47 | 53 | 5154 | 1.81 |
| 140000 | 62 | 38 | 6297 | 2.14 |
| 160000 | 56 | 44 | 7207 | 2.49 |
| 180000 | 50 | 50 | 7918 | 2.84 |
| 200000 | 49 | 51 | 9766 | 3.21 |

4 Summary

In this article we have shown that it is possible to construct three-dimensional Delaunay triangulations that can cope with a changing number of vertices as well as with moving vertices by using a very simple data structure. This data structure is obtained by adding neighborhood entries to every simplex and by storing the tetrahedra within a list. The performance of our data structure is comparable to that of more sophisticated data structures [1], which may pose an advantage for parallelization.

We have proposed a new incremental method of vertex deletion solving the serious problems in maintaining a valid three-dimensional Delaunay triangulation. We found that indeed by incrementally deleting a vertex from a Delaunay triangulation in a non-negligible fraction of cases the outside simplices (that were not incident to the deleted vertex) are affected by deletion. Numerical tests revealed our method of vertex deletion to be in practice faster than the

vertex insertion algorithm, since no simplex walk is necessary – this advantage usually compensates the higher effort required by the flips.

Note that the code allows to be generalized towards power-weighted Delaunay triangulations in a straightforward way by replacing the normal circum-sphere criterion by its weighted counterpart. In addition, the code already provides functionality to compute volumes and contact surfaces of the associated Voronoi cells which are of importance in some simulations of interacting particle systems. The generalization to Laguerre cells can also be done by replacing the center of the simplex circumspheres by its weighted counterpart. The resulting tessellation of space in Voronoi/Laguerre cells can be used to model growth/shrinking processes or for the numerical solution of differential equations on irregular grids. The first implementation of a vertex deletion algorithm for three-dimensional dynamic tessellations thus makes our code suitable for the simulation of dynamically interacting complex systems with variable particle numbers as e.g. cell tissues.

5 Acknowledgements

G. S. is indebted to T. Beyer for discussing many aspects of the algorithms and for testing the code and to U. Brehm for discussing many theoretical problems.

References

- [1] Jean-Albert Ferrez. *Dynamic triangulations for efficient 3d simulations of granular materials*. PhD thesis, EPFL, thesis 2432, 2001.
- [2] John von Neumann. *Theory of Self-Reproducing Automata*. University of Illinois Press, 1 edition, 1966.
- [3] R. M. Baer and H. M. Martinez. Automata and biology. *Ann. Rev. Biophys. Bioeng.*, 3:255–291, 1974.
- [4] Michael Meyer-Hermann. A mathematical model for the germinal center morphology and affinity maturation. *Journal of Theoretical Biology*, 216:273–300, 2002.
- [5] Frank Meineke, C.S. Potten, and Markus Loeffler. Cell migration and organization in the intestinal crypt using a lattice-free model. *Cell Proliferation*, 34:253–266, 2001.
- [6] Michael Weliky and George Oster. The mechanical basis of cell rearrangement. *Development*, 109:373–386, 1990.

- [7] Michael Weliky, George Oster, Steve Minsuk, and Ray Keller. Notochord morphogenesis in *xenopus laevis*: simulation of cell behavior underlying tissue convergence and extension. *Development*, 113:1231–1244, 1991.
- [8] Atsuyuki Okabe, Barry Boots, Kokichi Sugihara, and Sung Chiu. *Spatial Tessellations: Concepts and Applications of Voronoi Diagrams*. John Wiley and Sons, 1 edition, 1999.
- [9] Mark De Berg, Marc van Kreveld, Mark Overmars, and Otfried Schwarzkopf. *Computational Geometry*. Springer, Berlin, 1 edition, 1997.
- [10] Steven Fortune. Voronoi diagrams and delaunay triangulations. *Computing in Euclidean Geometry*, 1, 1992.
- [11] Christoph Lürig and Thomas Ertl. Adaptive iso-surface generation. *3D Image Analysis and Synthesis '96*, pages 183–190, 1996.
- [12] Gary L. Miller, Dafna Talmor, Shang-Hua Teng, and Noel Walkington. A delaunay based numerical method for three dimensions: generation, formulation, and partition. *Proceedings of the 27th Annual ACM Symposium on Theory of Computing*, pages 683–692, 1995.
- [13] Dean C. Bottino. Computer simulations of mechanochemical coupling in a deforming domain: applications to cell motion. *IMA Volumes in Mathematics and its Applications, Frontiers in Applied Mathematics Series*, 121:295–314, 2000.
- [14] E. Schönhardt. Über die Zerlegung von Dreieckspolyedern in Tetraeder. *Math. Annalen*, 98:309–312, 1928.
- [15] Jacob Goodman and Joseph O'Rourke. *Handbook of Discrete and Computational Geometry*. CRC Press, New York, 1 edition, 1997.
- [16] Gert Brouns, Alain De Wulf, and Denis Constales. Multibeam data processing: Adding and deleting vertices in a delaunay triangulation. *The Hydrographic Journal*, 101, July 2001.
- [17] Olivier Devillers. On deletion in delaunay triangulation. *Internat. J. Comput. Geom. Appl.*, 12:193–205, 2002.
- [18] H. Edelsbrunner and N. R. Shah. Incremental topological flipping works for regular triangulations. *Algorithmica*, 15:223–241, 1996.
- [19] Ernst Mücke. A robust implementation for three-dimensional delaunay triangulations. *International Journal of Computational Geometry and Applications*, 2(8):255–276, 1998.
- [20] Xue Xinjian, Righetti Franco, Telley Hubert, Th. M. Liebling, and Alain Mocellin. The laguerre model for grain growth in three dimensions. *Philosophical Magazine B*, 75(4):567–585, 1997.
- [21] Jörg Sauer. Allgemeine Kollisionserkennung und Formrekonstruktion basierend auf Zellkomplexen. Master's thesis, Universität des Saarlandes, Fachbereich 14 Informatik, 1995.

- [22] Charles Kittel. *Introduction to Solid State Physics, 7th Ed., Wiley, (1996)*. John Wiley and Sons, 7 edition, 1996.
- [23] F. Aurenhammer. Voronoi diagrams – a survey of fundamental geometric data structure. *ACM Computing Surveys*, 23(3):345–405, Sept. 1991.
- [24] Jean-Daniel Boissonnat and Monique Teillaud. On the randomized construction of the delaunay tree. *Theoretical Computer Science*, 112(2):339–354, 1993.
- [25] Taek J. Choi. Generating optimal computational grids: Overview and review. <http://www.me.cmu.edu/faculty1/shimada/cg97/taek/>, 1997.
- [26] Michael Allen Facello. Constructing delaunay and regular triangulations in three dimensions. Master’s thesis, University of Illinois at Urbana-Champaign, 1993.
- [27] O. Devillers. Improved incremental randomized Delaunay triangulation. In *Proc. 14th Annu. ACM Sympos. Comput. Geom.*, pages 106–115, 1998.
- [28] A. Bowyer. Computing dirichlet tessellations. *The Computer Journal*, 24(2):162–166, 1981.
- [29] Jean-Daniel Boissonnat and Mariette Yvinec. *Algorithmic Geometry*. Cambridge University Press, Cambridge, 1 edition, 1998.
- [30] Marc Vigo and Nuria Pla. Regular triangulations of dynamic sets of points. Technical report, 2000.